Effect of Cross-Linking on the Diffusion of Water, Ions, and Small Molecules in Hydrogels

Yanbin Wu, Sony Joseph, and N. R. Aluru*

Department of Mechanical Science and Engineering, Beckman Institute for Advanced Science and Technology, University of Illinois at Urbana−Champaign, Urbana, IL-61801

Received: September 12, 2008; Revised Manuscript Received: December 16, 2008

The present study reports on molecular dynamics investigations of chemically cross-linked poly(ethylene glycol) hydrogels with the aim of exploring the diffusion properties of water, ions, and rhodamine within the polymer at the molecular level. The water structure and diffusion properties were studied at various cross-linking densities with molecular weights of the chains ranging from 572 to 3400. As the cross-linking density is increased, the water diffusion decreases and the slowdown in diffusion is more severe at the polymer−water interface. The water diffusion at various cross-linking densities is correlated with the water hydrogen bonding dynamics. The diffusion of ions and rhodamine also decreased as the cross-linking density is increased. The variation of diffusion coefficient with cross-linking density is related to the variation of water content at different cross-linking densities. Comparison of simulation results and obstruction scaling theory for hydrogels showed similar trends.

Introduction

Hydrogels, composed of polymer networks and water, have been used increasingly in drug delivery systems, tissue engineering, contact lenses, and so forth[1−5] due to their interesting structural and mechanical properties. The solidlike character of the hydrogel system plays an important role by providing mechanical stability. The hydrogel system also maintains dynamic behavior typical of liquid phases.[5] Two properties of hydrogels, high water content and rubberlike nature, make them akin to a natural tissue. Biocompatibility and cross-linked structure are key properties of hydrogels that allow for various applications. Cross-linking allows immobilization of active agents and biomolecules and helps drug release at a well-defined rate. Cross-linking density is commonly used to tune key parameters like mesh size and molecular weight between cross-linkers in order to change macroscopic properties such as diffusion and Young's modulus. Among the dynamic properties, diffusion of small molecules, such as nutrients, is essential for vitality of living cells in biological systems.

In order to utilize hydrogels for various applications, it is essential to understand their material properties, flexibility, interactions with solutes and transport phenomena. A cross-linked network is difficult to be analyzed by experimental techniques of chromatography and fractionation owing to the network's inability to dissolve. Deeper insight into dynamic processes occurring within hydrogels have become possible by techniques such as high-flux neutron sources and X-ray synchrotrons.[6−8] Diffusion in hydrogel has been studied extensively using quasi-elastic neutron scattering (QENS),[9,10] NMR,[11−13] side-by-side diffusion cells,[14] fluorescence correlation spectroscopy,[15,16] refractive index method,[17] and so forth.

Many physical models have been developed to model the diffusion of small solutes in hydrogels.[18,19] Solute behavior in hydrogels has been explained in terms of reduction in hydrogel free volume,[20−22] enhanced hydrodynamic drag on the solute,[23,24] increased path length due to obstruction,[25,26] and a combination of hydrodynamic drag and obstruction effects.[27] The theoretical relations are limited and rely on fitting parameters that are typically not known. With the rapid development of molecular dynamics simulation techniques, it is now possible to study the structure and dynamics of biomacromolecular systems in an aqueous environment considering explicit water, ion, and solute molecules.[28,29] In recent times, molecular dynamics simulation has been used to study physical gels,[30] poly(vinyl alcohol),[10,31] poly(vinyl methyl ether),[32] poly(*N*-isopropylacrylamide),[32] polyacrylamide,[33] epoxy-amine networks,[34] and so forth. Structure and dynamics of the polymer−water interface in poly(vinyl alcohol) (PVA) for a mesh size of 1 nm was studied recently.[10] Solvent diffusion coefficient and residence times in hydrophilic systems indicate that water behaves as a supercooled liquid phase.[10] Structural and mechanical properties and diffusion of glucose and vitamin D in poly(ethylene glycol) (PEG) and poly(acrylic acid) (PAA) and their double network was investigated by Jang et al.[35] Effects of confined water in cages of different chemical and structural features have also been investigated previously in other natural and man-made structures such as vycor glass,[36] carbon nanotubes,[37,38] boron-nitride nanotubes,[39] zeolites,[40] cellular membrane channels,[41] proteins,[29] carbohydrate solution,[42] and so forth.

Poly(ethylene glycol) (PEG)-based hydrogel network has been increasingly utilized in tissue engineering applications in recent years. This is mainly due to their hydrophilicity and resistance to protein adsorption and biocompatibility. They can also be customized by modifying the chain length and adding biological functional groups. Besides, PEG hydrogel is a promising membrane material for selective removal of CO_2 from a mixture containing light gases such as CH_4, N_2 and H_2.[43] PEG can be easily cross-linked using acrylate group as a cross-linker. In conventional polymerization, the cross-linking density, defined as the number of cross-linkers divided by the number of monomers, need not be homogeneous throughout the network, but in poly(ethylene glycol) diacrylate (PEGDA) it is homogeneous because the molecular weight between the cross-linkers is the same as that of the PEG monomer. This enables PEGDA to be used as an ideal material for studying gel properties. Since

* To whom correspondence should be addressed. E-mail: aluru@illinois.edu.

10.1021/jp808145x CCC: $40.75
Published on Web 02/24/2009

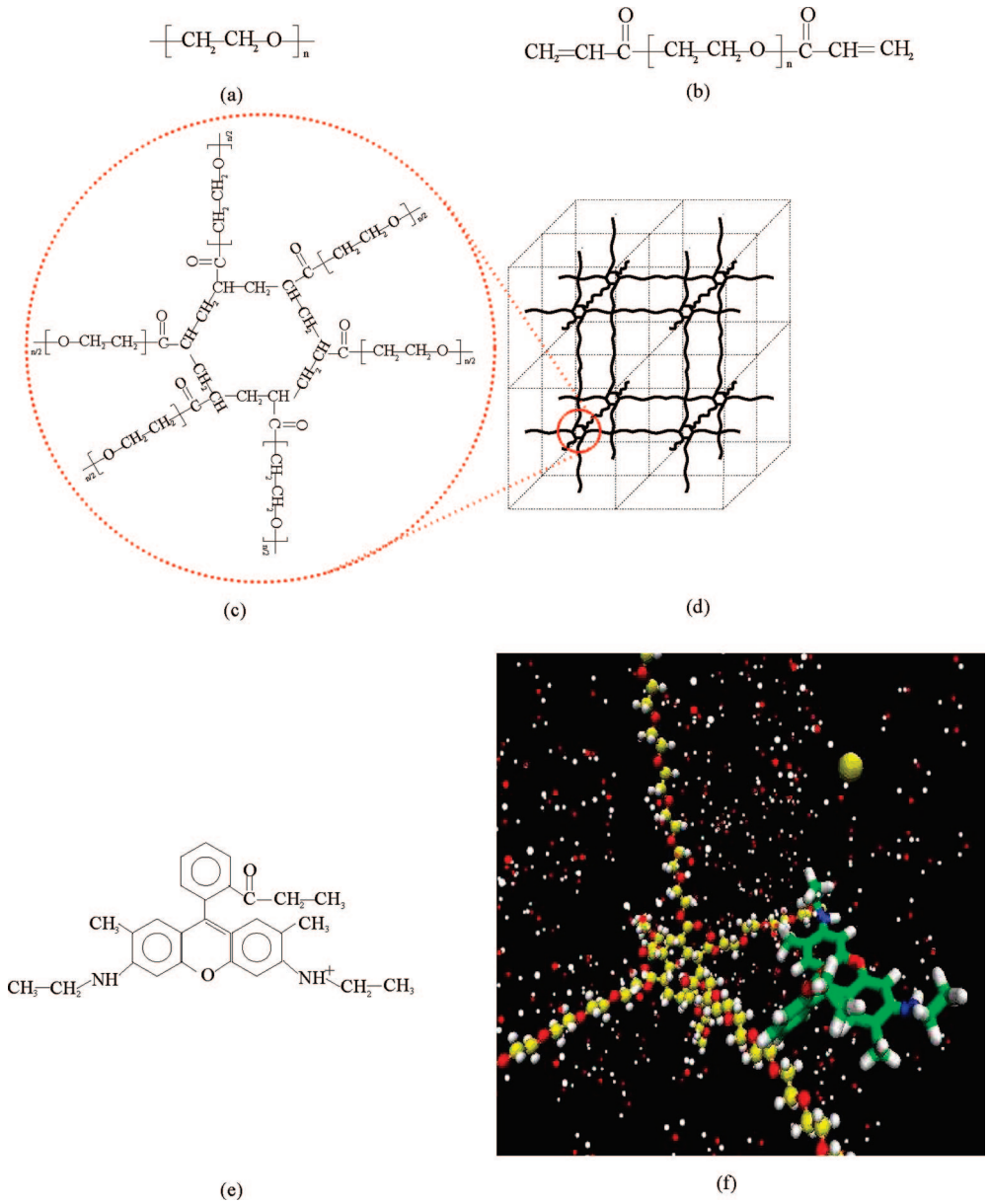

Figure 1. (a) Chemical structure of PEG. (b) Chemical structure of PEGDA. (c) 6 PEGDA chain ends meet and form cyclododecane as cross-linking point. (d) Cross-linked network with 2 × 2 × 2 cells in three dimensions. (e) Chemical structure of rhodamine. (f) Visualization of simulation box with polymer network, water, rhodamine, and chloride molecules. Yellow, carbon; red, oxygen; white, hydrogen.

TABLE 1: System Composition and Equilibrated Mesh Size[a]

prepolymer	PEG572	PEG1000	PEG1500	PEG2000	PEG3400
n	13	23	34	45	78
cross-linking density(1/*n*)%	7.69	4.35	2.94	2.22	1.28
equilibrated water content/%	74.7	84.2	85.5	89.9	90.9
polymer volume content/%	25.3	15.8	14.5	10.1	9.1
mesh size/nm	2.28	3.14	3.64	4.47	5.49
number of water molecules per cell	291	855	1353	2636	4984
number of cells	2 × 2 × 2	2 × 2 × 2	2 × 2 × 2	1 × 1 × 1	1 × 1 × 1
simulation box size/nm	4.56	6.28	7.28	4.47	5.49

[a] *n* is the degree of polymerization before cross-linking. Mesh size is a function of *n*.

cross-linking has a significant impact on the structural and dynamic properties of the hydrogel, we investigate the structural and dynamic properties of a hydrogel consisting of cross-linked PEGDA, water, and small solutes (ions and rhodamine) using molecular dynamics (MD) simulations, as they can provide a useful description of water and solute mobility by considering explicit water and partial charge for PEG atoms. Rhodamine is commonly used as a tracer dye in experiments within hydrogel networks to determine the transport properties of the network. Studying rhodamine diffusion also helps to understand the diffusion of similar sized biomolecules in PEGDA.

The rest of the paper is organized as follows: first, we present the system setup with the force fields used and a description of the construction of the cross-linked structure. Then we inves-

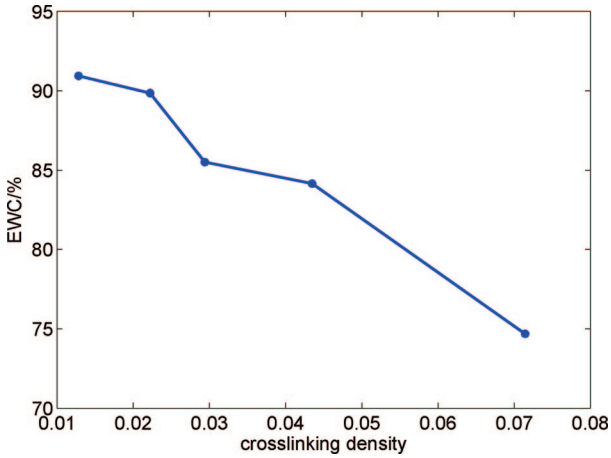

Figure 2. Equilibrated water content (EWC) used in the simulations for different cross-linking densities. EWC is the volume fraction of water in the simulation box.

tigate the water structure and hydrogen bonding in various regions divided according to the distance from the polymer. Next, we present the results and discussion on the variation of diffusion coefficients of water, ions, and rhodamine as a function of the cross-linking density. Finally, we compare the variation of diffusion coefficient with cross-linking density from MD simulation results with the variation predicted from Amsden obstruction scaling theory.

Methods

Force Field. A force field of the following form has been employed

$$E_{\text{total}} = E_{\text{vdW}} + E_{\text{Q}} + E_{\text{bond}} + E_{\text{angle}} + E_{\text{dihedral}} \quad (1)$$

where E_{total}, E_{vdW}, E_{Q}, E_{bond}, E_{angle}, and E_{dihedral} are the total, van der Waals (vdW), electrostatic, bond stretching, angle bending, and torsion energies, respectively. In our simulations, we used the all atom force field. The force field parameters and charges for the PEG chain are taken from Smith et al.,[44] Lennard-Jones (LJ) interaction parameters between PEG and water are taken from Bedrov et al.,[45] rhodamine are taken from Vaiana et al.,[46] and the acrylate cross-linker, chloride, and sodium ions are from the CHARMM27 force field.[47] For water, we used the single point charge/extended (SPC/E) model.[48] In order to verify the interaction parameters between PEG and water, we simulated a system composed only of PEG chains and water and calculated the radial distribution function of the oxygen of the PEG with the oxygen of water and obtained good agreement with the results of Borodin et al.[49] For cross LJ interaction parameters between rhodamine and water, we used Lorentz−Berthelot combination rules and validated by calculating the diffusion coefficient of rhodamine in bulk water. We obtained a diffusion coefficient of 0.4243×10^{-5} cm^2/s which is within the range of values obtained in various experiments (0.3×10^{-5} to 0.5×10^{-5} cm^2/s).[50−52] For cross LJ interaction parameters between ions and water and between PEG chain and CHARMM atoms, we followed Patra et al.[53] and Zheng et al.,[54] respectively, and used Lorentz−Berthelot combination rules.

Simulation System Setup. For our simulations, we used a cross-linked PEGDA structure with an ideal network without any free dangling ends or self-looping or entanglements. Figure 1a shows a PEG chain with n monomers. Each PEGDA molecule (see Figure 1b) is a PEG chain connected to acrylate groups at both ends that serve as cross-linkers. Under the influence of ultraviolet rays, the acrylate double bond breaks and connects with other PEG chains (see Figure 1c) to form the cross-linking point. We used an ideally cross-linked unit cell where six PEGDA chains meet at the cross-linking point, forming a cyclododecane ring structure at the unit cell center (see Figure 1c,d), similar to the approach presented by Jang et al.[35] The cross-linking density is defined as the number of cross-linkers (acrylate groups at the ends) divided by the number of monomers (ethylene glycol). For ideal cross-linking, the cross-linking density is $1/n$, where n is the degree of polymerization of the PEG chain. The higher the degree of polymerization of the PEG chain, the lower is the cross-linking density. The ideally cross-linked unit cell was periodically replicated along xyz-directions, forming a three-dimensional (3D) hydrogel simulation box, as shown in Figure 1d. We systematically built gels with different cross-linking densities and investigated diffusion of water and small solutes in these gels. Table 1 shows the different cross-linking density cases we considered. The cross-linked PEGDA structures were then solvated by water. We chose the number of water molecules to insert into the system based on experimental measurements. Using results of Padmavathi et al.,[55] which gives the equilibrium water content for a wide range of cross-linking densities, we calculated the number of water molecules to insert into the system. The swelling ratios in experiments were for a prepolymer PEG solution of around 30% w/w concentration. The equilibrated water content (EWC) used in our system is given in Table 1. EWC is defined as the ratio of the volume of water in the simulation box to the total volume of the simulation box. Figure 2 depicts the EWC data in graphical form. We also compared the water content we used against several other papers[11,56−59] that had some of the cross-linking densities that we considered and found our numbers to be reasonable. For the case with ions, we assumed that the number of water molecules remained the same even after adding ions such that there was essentially no swelling after we inserted ions into the system. The NaCl ion concentration considered was 0.5 M within the gel. For the rhodamine case, we had to consider the fact that if the concentration of rhodamine was above 10^{-6} M, typically rhodamine aggregation occurred by

TABLE 2: Average Coordination Number for Different Cross-Linking Densities

prepolymer	$n = 13$	$n = 23$	$n = 34$	$n = 45$	$n = 78$
	0.6792	1.0118	1.0382	1.4894	1.5985

TABLE 3: The Average Number of Hydrogen Bonds Per Water Molecule in Each Region for Different Cross-Linking Densities[a]

prepolymer	I (total)	II	III	IV	I (water−water)
$n = 13$	3.29	3.51	3.57		2.90
$n = 23$	3.34	3.55	3.58	3.58	2.94
$n = 34$	3.35	3.55	3.58	3.58	2.95
$n = 45$	3.38	3.56	3.59	3.59	2.98
$n = 78$	3.40	3.57	3.59	3.59	3.00

[a] The last column shows water−water hydrogen bonding in region I, not including polymer−water hydrogen bonding. Regions II, III, and IV do not have any polymer−water HB. For region IV, at the highest cross-linking density $n = 13$ there is no bulk region IV.

TABLE 4: Number of Hydrogen Bonds Per Polymer Ether Oxygen for Different Cross-Linking Densities in Region I

prepolymer	$n = 13$	$n = 23$	$n = 34$	$n = 45$	$n = 78$
	0.716	0.721	0.716	0.721	0.719

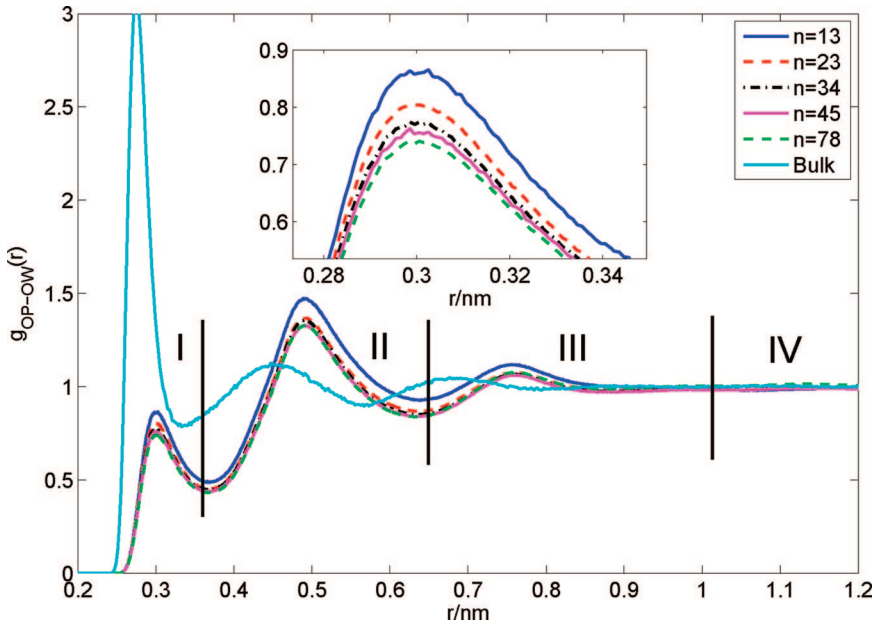

Figure 3. RDF between oxygens of polymer ether and oxygen of water and between water oxygens in bulk water. Inset: amplification of the first peak. The RDF, $g_{OP-OW}(r)$, can be computed by normalizing the local density of water molecules at a distance of r from the polymer ether oxygens with the average density of water molecules in the total system. Water is divided into regions I, II, III, and IV according to the distance from the polymer.

stacking up on its three-ring xanthylium plane (rhodamine structure is shown in Figure 1e) and this hindered fluorescent yield and diffusion. In experiments, to avoid aggregation a very dilute solution is used, but in simulations, such low concentrations would need an extremely large box size and would be computationally expensive. So in our simulations, we used only one rhodamine in the system with the simulation box size ranging from 4.56 to 7.28 nm, which is much larger than 4 Å, the distance between the planes of rhodamine molecules in a dimer structure formed during aggregation.[60] The final system composition and equilibrated mesh size for the different cases are summarized in Table 1. Figure 1f shows a snapshot of the simulation box comprising of the polymer network, water, rhodamine, and chloride ions.

MD simulations were performed with Gromacs 3.3.1.[61] Time integration was performed using the leapfrog algorithm with a time step of 1.0 fs. The short-range vdW interactions were computed using a cutoff scheme (cutoff distance, 1.0 nm). The long-range electrostatic interactions were computed by using a particle mesh Ewald method[61] (real space cutoff, 1.0 nm; FFT grid spacing, 0.12 nm, fourth-order interpolation). The Nose−Hoover thermostat[62,63] with a time constant of 0.5 ps was used to maintain the temperature at 300 K. We built the polymer network with all PEG chain segments in an all-trans conformation first and then inserted water molecules according to equilibrated water content in the hydrogel. After that, we let the system equilibrate for 1 ns in an NPT ensemble by maintaining a pressure of 1 bar (compressibility time constant of 0.2 ps; compressibility of 4.5×10^{-5} bar^{-1}) with a Parrrinello−Rahman barostat.[64] The energy, temperature, and box size of the simulation box reached constant values during this equilibration process. Then we further equilibrated the system for additional 1 ns of simulation time using an NVT ensemble at 300 K. The energy and temperature of the simulation box reached constant values during this equilibration process. The resulting configuration is used as the starting point for further simulations. For collecting sufficient statistics to compute various properties, the simulations were run for 54 ns.

Polymer−Water Interaction and Water Dynamics

Radial Distribution Function between Polymer and Water. The radial distribution function (RDF) $g(r)$ gives the probability density of finding a particle at a distance r from a given particle position. Because the PEG molecules are somewhat immobilized by cross-linkers as compared to the solvent, the water molecules that are close to PEG are expected to have much slower translational and rotational dynamics than water far away from PEG, similar to the behavior observed in confining environments[65,66] and around biomacromolecules such as proteins[67−69] and DNA.[70−72] From an inspection of the radial distribution function between polymer ether oxygen and water oxygen, as shown in Figure 3, the perturbation of the water distribution around PEG ether groups, relative to the average water density, extended to a radius of about 1.04 nm from the polymer ether oxygen. The water around a PEG ether oxygen is less structured than water around a bulk water molecule. The RDFs here are similar to the RDFs between water and polymer oxygens for polymer−water solutions (PEO530 and 1,2-dimethoxyethane) with 17% polymer weight percentage.[73] For different cross-linking densities, the peak positions of the RDFs between polymer ether oxygen and water oxygen are essentially the same (see Figure 3). As cross-linking density increases, the value of the first peak increases slightly (see Figure 3 inset). The number of water oxygens per PEG ether oxygen, or the average coordination number, n_{OP-OW}, can be evaluated by the following equation:

$$n_{OP-OW} = \frac{N_{OW}}{V_{box}} \int_0^{R_{min}} 4\pi r^2 g_{OP-OW}(r) dr \qquad (2)$$

where N_{OW} is the total number of water oxygens in the box, V_{box} is the volume of the box and R_{min} is the position of the first valley. The average coordination number is summarized in Table 2. The coordination number decreases as the cross-linking density increases. This implies that fewer water molecules come close to the polymer when cross-linking density increases and water content decreases. The variation of coor-

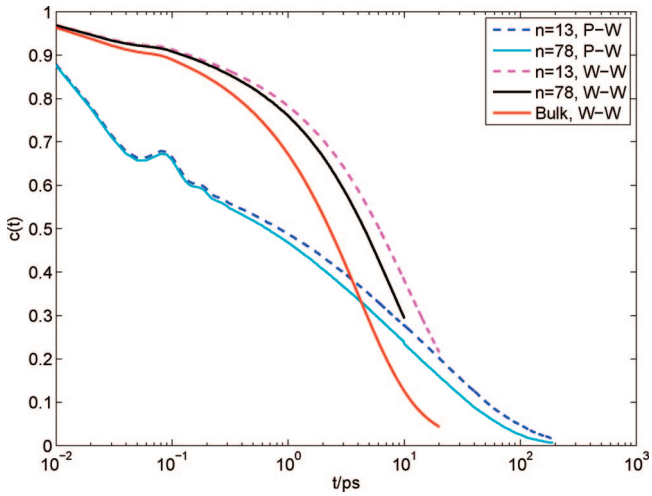

Figure 4. Decay of autocorrelation function $c(t)$ for polymer−water (P−W) and water−water (W−W) hydrogen bonding in region I. The autocorrelation function for the lowest ($n = 78$) and the highest ($n = 13$) cross-linking density cases are shown.

dination number shown here is similar to the phenomenon observed in 1,2-dimethoxyethane/water solutions with varying polymer concentration.[74]

The water molecules in the gel system can be assigned into different regions according to their distance from the polymer ether oxygen atoms. We sampled the solvent in different regions, according to the $g_{OP-OW}(r)$ behavior.[10] Since there are three peaks in the curve, we divided the water into four regions. Region I ($r < 0.36$ nm) and region II (0.36 nm $< r <$ 0.64 nm) are considered as "close contact" regions. Water at distances between 0.64 and 1.04 nm, where the perturbation in the $g_{OP-OW}(r)$ was minor, is chosen as region III. The remaining water molecules are considered to be region IV. Water molecules in regions I−IV are characterized in terms of hydrogen bonding, relaxation times, and diffusion coefficients.

Water Hydrogen Bonding. The hydrogen bonding (HB) structure between water molecules and that between PEG ether oxygen and water was studied by analyzing the trajectory. Hydrogen bonding is defined by adopting the geometric criteria where the acceptor−donor (O···O) distance is less than 0.35 nm and the angle (O−H···O) is less than 30°. For each cross-linking density across different regions, the total number of hydrogen bonds is fairly constant except for a small dip in region I, as shown in Table 3. In region I, the water−water hydrogen bonding is lowered, but that is made up for to some extent by the hydrogen bonding with the polymer ether oxygen which acts as an acceptor (see Table 4). The variation of the number of hydrogen bonds across different regions is similar to that seen in simulations of PVA hydrogels.[10] As cross-linking density increases, HB per water molecule decreases for all regions. For the highest cross-linking density case ($n = 13$), there is no bulk region and region IV is undefined.

Hydrogen Bond Dynamics. The intermittent time autocorrelation function $c(t)$ expresses the probability that a randomly chosen pair of molecules is bonded at time t, provided that a bond existed at time $t = 0$, regardless of whether it was bonded in the interim time. $c(t)$ provides valuable insight into the relaxation of the system's H-bonding network. $c(t)$ is given by

$$c(t) = \frac{\langle h(t)h(0)\rangle}{\langle h(0)h(0)\rangle} \tag{3}$$

where $h(t)$ is 1 if molecules are bonded at time t and 0 if not. $\langle\rangle$ denotes average over all pairs of HB at $t = 0$ and over many

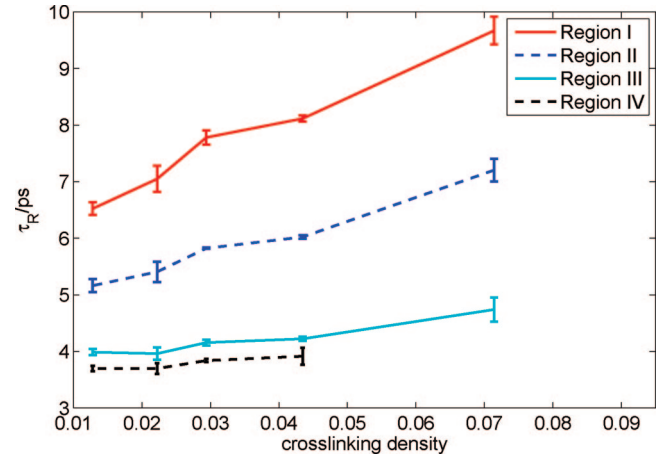

Figure 5. The relaxation time τ_R from the stretched exponential fit of the water−water HB autocorrelation function in regions I, II, III, and IV.

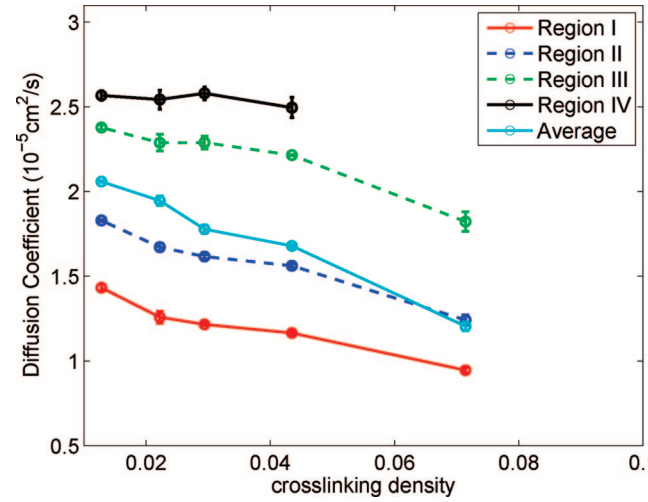

Figure 6. Diffusion of water in different regions as a function of the cross-linking density of the gel.

time steps. Figure 4 shows the hydrogen bond autocorrelation functions for various cross-linking densities and bulk water. The decay can be divided into two parts: short time relaxations within the librational regime (<0.1 ps) and long time relaxations beyond 0.1 ps. Water−water hydrogen bonding in the gel for $n = 78$ decays slower than the decay of water−water hydrogen bonding in the bulk. At the highest cross-linking density considered ($n = 13$), the decay is even slower. Compared to the water−water hydrogen bonding in the gel, the decay of the polymer−water hydrogen bonding shows different characteristics; polymer−water hydrogen bonds decay faster in the short time and is slower in the long time regime.

The long-time hydrogen bond dynamics is not characterized by an exponential relaxation with a single relaxation time τ_R,[75] but by a stretched exponential function with a stretch parameter β as well[76]

$$c(t) \approx A_0 \exp[-(t/\tau_R)^{\beta}] \tag{4}$$

Stretched exponential function fit is considered to be purely empirical in most cases, but some physical significance may be attached to it for water. For bulk water, at room temperature, the physical origin of this stretched exponential at long times can be understood in terms of the coupling of hydrogen bond dynamics to diffusion.[77] In our cross-linked PEGDA systems,

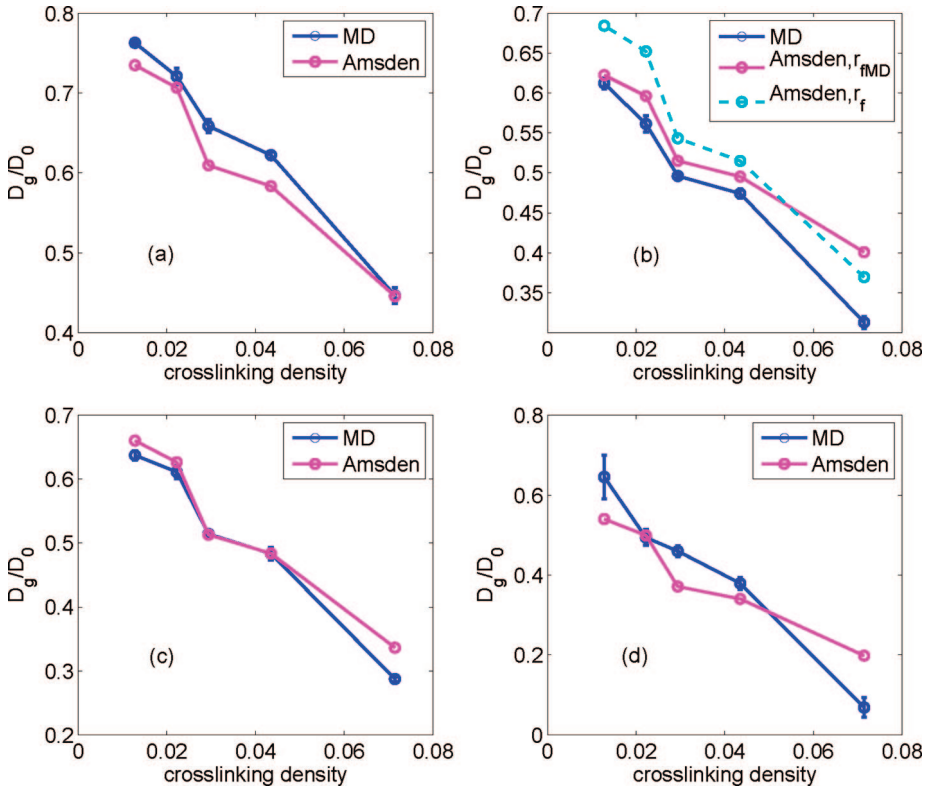

Figure 7. Normalized diffusion of water, ions, and rhodamine as a function of cross-linking density obtained using molecular dynamics and theoretical prediction. The diffusion coefficient D_g is normalized with respect to the diffusion coefficient in bulk water D_0. Diffusion of (a) water, (b) chloride ion, (c) sodium ion, and (d) rhodamine. For chloride ion, polymer fiber radius based on MD radial distribution function, $r_{fMD} = 0.5535$ nm, is used instead of r_f calcuated from eq 7.

we found that the stretched exponential parameters $\beta \approx 0.64$ and $A_0 \approx 1.0$ were almost independent of the cross-linking density. From the relaxation times τ_R calculated for different cross-linking densities (see Figure 5), it is evident that hydrogen bonds between water molecules survive longer when water is close to the polymer, similar to the observations in PVA hydrogels.[10] With increasing cross-linking density, the relaxation times of the hydrogen bonds increase as well. The results of the hydrogen bonding dynamics indicate that the existence of polymer leads to an overall slowing down of the system dynamics, and this slow-down is more severe as the cross-linking density increases. To quantify the slowdown, we calculate the water diffusion coefficients in different regions for different cross-linking densities.

Diffusion Coefficients. The diffusion coefficients for water, ions, and rhodamine, D, were obtained from the long-time slope of the mean square displacement

$$D = \frac{1}{6}\lim_{t\to\infty}\frac{d}{dt}\langle|\mathbf{r}(t) - \mathbf{r}(0)|^2\rangle \qquad (5)$$

where $\mathbf{r}(t)$ and $\mathbf{r}(0)$ are the position vectors of the center of mass at time t and 0, respectively, with an average performed over the simulation time and over all the number of molecules. For water, to evaluate the limiting slope, we considered a time window equal to the average lifetime of the HB between PEG ether groups and water. The time evolution of this interaction is shown in Figure 4, where the time autocorrelation function of the hydrogen bonds, $c(t)$ is reported. The correlation time, t^*, was obtained by integrating polymer−water $c(t)$. t^* could be considered as the highest limiting value for the residence time in a particular region of a water molecule. The computed value of t^* varied between 10 to 20 ps depending on the cross-linking density. The results of the diffusion coefficient for each region are summarized in Figure 6. The error bar in the plot is the standard deviation of the diffusion coefficients based on three trajectories for the same system with different initial configuration. The average water diffusion decreases as the cross-linking density increases, similar to the observations in poly(*N*-isopropylacrylamide) hydrogel[13] and in poly(methacrylic acid) hydrogel.[78] For each cross-linking density, water diffusion coefficient decreases as it approaches the polymer−water interface. The variation of the diffusion coefficient of water with cross-linking density is similar to the variation of the equilibrium water content shown in Figure 2.

The diffusion coefficients of ions as a function of cross-linking density are shown in Figure 7b,c. For an ion concentration of 0.5 M, we observe that the diffusion of ions decreases as cross-linking density increases. Similar to the water case, ion diffusion also follows the water content variation with cross-linking density. Lobo et al.[79] studied diffusion of potassium chloride and lithium chloride in acrylamide hydrogels and found that electrolyte diffusion depends on water content inside the polymer matrix. The results of our ion diffusion are comparable with experimental results for potassium chloride (KCl) and lithium chloride (LiCl) diffusion in hydrogels; for 1% cross-linking density acrylamide hydrogel with the same ion concentration, diffusion coefficients of KCl and LiCl within the gel are 31.9 and 42.7% of their values in aqueous solution.

To calculate the translational diffusion coefficient of rhodamine, we first estimated the rotational relaxation time of rhodamine. Rotational relaxation time is obtained from the relaxation time of the autocorrelation function $\langle\mathbf{n}(t)\cdot\mathbf{n}(0)\rangle$, where $\mathbf{n}(t)$ is the vector normal to the xanthylium plane of the rhodamine molecule. The computed rotational relaxation time of around

TABLE 5: Physical Properties of the Hydrogel Used in Amsden's Obstruction Scaling Theory

M_m (g/mol)	υ (cm^3/g)	l (nm)	a (nm)	r_f (nm)	C_∞	χ
44	0.8453[57]	0.36	1.54	0.2337	5.2[87]	0.46[87]

200 ps is comparable to the 100−200 ps in experiments.[80] A time window of 400 ps, a much larger value than the rotational relaxation time was used to compute the slope of the mean square displacement. Diffusion of rhodamine decreases with increasing cross-linking density, which is similar to the trend observed for water and ions, as shown in Figure 7d. To accurately compute the diffusion coefficient with a linear MSD plot, 54 ns of simulation time was required. The diffusion coefficient of rhodamine in bulk water was 0.4243×10^{-5} cm^2/s. For the highest cross-linking density considered rhodamine diffusion is less than 5% of the bulk value.

Our results are comparable to the diffusion of molecules of similar size in PEGDA gels in literature. Jang et al.[35] built PEG(1300)DA hydrogel system and studied diffusion of two small solute molecules, D-glucose and ascorbic acid (vitamin C). The diffusion coefficient of D-glucose in the gel was reported as $0.173 \pm 0.050 \times 10^{-5}$ cm^2/s, which is one-third of the D-glucose diffusion in water ($0.6 - 0.7 \times 10^{-5}$ cm^2/s).[81−83] D-glucose has a hydrodynamic radius of 3.61−3.8 Å,[84,85] that is comparable to 0.53 ± 0.03 nm of rhodamine 6G.[86] Using fluorescence correlation spectroscopy, Watkins et al.[15] studied diffusion of fluorescent probes Cl-NERF and Texas Red sulfonyl chloride, which have a hydrodynamic radius of 0.7 nm, in PEG(700)DA and PEG(1000)DA hydrogel. They obtained diffusion coefficients on the order of 10^{-8} cm^2/s.

Comparison with Theory. Over the years, several theoretical models have been developed to characterize diffusion of solutes in hydrogels. Amsden[18] compares several theories and models for solute diffusion within hydrogels and suggests Amsden's theory where hydrodynamic models are combined with obstruction models as one of the best theories that matched several experimental results. According to the obstruction scaling theory,[87,88] the diffusion as a function of the polymer volume fraction is

$$\frac{D_g}{D_0} = \exp\left[-\pi\left(\frac{r_s + r_f}{k_s a \varphi^{-0.75} C_\infty^{-0.25}(1 - 2\chi)^{-0.25} + 2r_f}\right)^2\right] \quad (6)$$

where a is the equivalent bond length of the monomer, ϕ is the polymer volume fraction, r_s is the radius of solute, r_f is the radius of polymer chain, C_∞ is the characteristic ratio of polymer, χ is the Flory−Huggins polymer/solvent interaction parameter, D_g is the diffusion coefficient of solute in gel, and D_0 is the diffusion coefficient of solute in water calculated from MD simulation and verified by literature.[38,50−52,89] Since the fitting parameter $k_s \simeq 1$ for the different polymers and solutes considered, Amsden proposed this model as a "universal" model for solute diffusion in hydrogels. The radius of the polymer chain is given by[87]

$$r_f = \left(\frac{M_m \upsilon}{l\pi N_A}\right)^{1/2} \quad (7)$$

where l is the length of the monomer unit, M_m is the molecular weight of the monomer, υ is the specific volume of the polymer, and N_A is the Avogadro number. The solute size r_s is the hydrodynamic radius of the solute computed by the Stokes−Einstein relation[87]

$$r_s = \frac{k_B T}{f\pi\eta D_0} \quad (8)$$

where k_B is Boltzmann's constant, η is the viscosity of water at temperature T, and f is 4 for solutes whose size approaches that of the solvent (i.e., water) and 6 for solutes greater in size than the solvent.[90]

We compared our molecular dynamics simulation results with that from Amsden's obstruction scaling theory. The parameters used in eq 6 are listed in Table 5. According to Koneshan et al.[91] and Valente et al.,[92] Stokes' law breaks down for small ions in highly polar solvents. Nightingale[93] extended the empirical correction to Stoke's law to provide a set of modified hydrodynamic radii for small ions. In using Amsden's theory, we used the modified hydrodynamic radii from Nightingale[93] for water, sodium, and chloride ions rather than using the Stokes−Einstein relation. For rhodamine, we followed the same procedure as Jang et al.[35] to compute the hydrodynamic radius

$$\langle r_h \rangle^{-1} = \frac{1}{N^2}\sum_{j\neq i}^{N}\sum_{i=1}^{N}\left\langle\frac{1}{r_{ij}}\right\rangle \quad (9)$$

where N is the number of atoms in the rhodamine molecule, and r_{ij} is the distance between two atom pairs. The solute size r_s we used for water, sodium ion, chloride ion, and rhodamine are listed in Table 6. For comparison, the hydrodynamic radii from the Stokes−Einstein relation are also listed.

In Figure 7 we compare the results from our MD simulations with the prediction from Amsden's theory for water and the different solutes we considered. Diffusion data for water and sodium ion match better than that of chloride ion. The difference could be from the fact that the equation for calculating the radius of the polymer fiber, eq 7 does not take the ion size differences, and the different distances of closest approach into account. For the sodium ion, the first peak from the radial distribution function between oxygen of the polymer and the sodium ion was close to the value obtained from eq 7, but for the chloride ion, the first peak was at 0.5535 nm. Therefore we used 0.5535 nm as r_f for chloride ion.

Even though there is no perfect match, the theory matches reasonably well with MD results. As mentioned previously, the shapes of all the diffusion data are similar, and they follow the shape of the equilibrated water volume fraction, as shown in Figure 2. Unless the solute size and mesh size are comparable, such that the molecular level structure of the polymer network and the solute structure affect the diffusion, it is the equilibrated water content that is the key parameter in determining the diffusion coefficient. In experiments, factors, such as concentration of prepolymer solution, defects, rate of gelation, and so

TABLE 6: Hydrodynamic Radii and Modified Hydrodynamic Radii Used in This Work for Water, Ions, and Rhodamine

solute	water	chloride ion	sodium ion	rhodamine
bulk diffusion coefficient/$\times 10^{-5}$ cm^2/s	2.70[38]	1.85[89]	1.32[89]	0.4243[50−52]
hydrodynamic radius (nm)	0.0914	0.1335	0.1870	0.5819
radius used in this work (nm)	0.276	0.332	0.358	0.4873

forth, influence the final gel structure and thus the equilibrated water content and the diffusion data.

Conclusions

To summarize, we have presented molecular dynamics investigations of diffusion of water and small solutes in PEGDA hydrogels of varying cross-linking densities. Diffusion coefficient of water and small solutes decreases as cross-linking density increases. The decrease in diffusion of water is correlated with the increase in hydrogen bonding relaxation times. The simulation results compare well with Amsden's obstruction scaling theory, if the hydrodynamic radii of the solutes can be computed more accurately than from the Stokes- Einstein relation. The diffusion behavior corresponds quite well with the equilibrated water content in each gel.

Acknowledgment. This work was supported by NSF under Grants 0120978 (Water CAMPWS, UIUC), 0328162 (nano-CEMMS, UIUC), 0523435, and 0810294.

References and Notes

(1) Peppas, N. A.; Huang, Y.; Torres-Lugo, M.; Ward, J. H.; Zhang, J. *Annu. Rev. Biomed. Eng.* **2000**, *2*, 9–29.
(2) Lee, K.; Mooney, D. *Chem. Rev.* **2001**, *101*, 1869–79.
(3) Byrne, M.; Park, K.; Peppas, N. *Adv. Drug Deliv. Rev.* **2002**, *54*, 149–161.
(4) Langer, R.; Peppas, N. *AIChE J.* **2003**, *49*, 2990–3006.
(5) Underhill, G.; Chen, A.; Albrecht, D.; Bhatia, S. *Biomaterials* **2007**, *28*, 256–270.
(6) Gabel, F.; Bicout, D.; Lehnert, U.; Tehei, M.; Weik, M.; Zaccai, G. *Q. Rev. Biophys.* **2003**, *35*, 327–367.
(7) Winter, R. *Biochem. Biophys. Acta* **2002**, *1595*, 160–184.
(8) Koch, M.; Vachette, P.; Svergun, D. *Q. Rev. Biophys.* **2003**, *36*, 147–227.
(9) Paradossi, G.; Cavalieri, F.; Chiessi, E.; Telling, M. *J. Phys. Chem. B* **2003**, *107*, 8363–8371.
(10) Chiessi, E.; Cavalieri, F.; Paradossi, G. *J. Phys. Chem. B* **2007**, *111*, 2820–2827.
(11) Cruise, G.; Scharp, D.; Hubbell, J. *Biomaterials* **1998**, *19*, 1287–1294.
(12) Yasunaga, H.; Kobayashi, M.; Matsukawa, S.; Kirosu, H.; Ando, I. *Annu. Rep. NMR Spectrosc.* **1997**, *34*, 40–105.
(13) Tanaka, N.; Matsukawa, S.; Kurosu, H.; Ando, I. *Polymer* **1998**, *39*, 4703–4706.
(14) Stringer, J.; Peppas, N. *J. Controlled Release* **1996**, *42*, 195–202.
(15) Watkins, A.; Anseth, K. *Macromolecules* **2005**, *38*, 1326–1334.
(16) Russell, R.; Axel, A.; Shields, K.; Pishko, M. *Polymer* **2001**, *42*, 4893–4901.
(17) Weng, L.; Zhou, X.; Zhang, X.; Zhang, L.; Xu, J. *Macromol. Rapid Commun.* **2002**, *23*, 968–971.
(18) Amsden, B. *Macromolecules* **1998**, *31*, 8382–8395.
(19) Masaro, L.; Zhu, X. *Prog. Polym. Sci.* **1999**, *24*, 731–775.
(20) Yasuda, H.; Peterlin, A.; Colton, C. K.; Smith, K. A.; Merrill, E. W. *Makromol. Chem.* **1969**, *126*, 177–186.
(21) Peppas, N.; Reinhart, C. *J. Membr. Sci.* **1983**, *15*, 275–287.
(22) Lustig, S.; Peppas, N. *J. Appl. Polym. Sci.* **1988**, *36*, 735–747.
(23) Cukier, R. *Macromolecules* **1984**, *17*, 252–255.
(24) Phillips, R.; Deen, W.; Brady, J. *AIChE J.* **1989**, *35*, 1761–1769.
(25) Ogston, A. *Trans. Faraday Soc.* **1958**, *54*, 1754–1757.
(26) Johansson, L.; Elvingson, C.; Loefroth, J. *Macromolecules* **1991**, *24*, 6024–6029.
(27) Johnson, E.; Berk, D.; Jain, R.; Deen, W. *Biophys. J.* **1996**, *70*, 1017–1023.
(28) Hansson, T.; Oostenbrink, C.; van Gunsteren, W. *Curr. Opin. Struct. Biol.* **2002**, *12*, 190–196.
(29) Bizzarri, A.; Cannistraro, S. *J. Phys. Chem. B* **2002**, *106*, 6617–6633.
(30) Tamai, Y.; Tanaka, H.; Nakanishi, K. *Macromolecules* **1996**, *29*, 6750–6760.
(31) Tamai, Y.; Tanaka, H. *Chem. Phys. Lett.* **1998**, *285*, 127–132.
(32) Tamai, Y.; Tanaka, H. *Fluid Phase Equilib.* **1998**, *144*, 441–448.
(33) Netz, P.; Dorfmuller, T. *J. Phys. Chem. B* **1998**, *102*, 4875.
(34) Mijovic, J.; Zhang, H. *J. Phys. Chem. B* **2004**, *108*, 2557–2563.
(35) Jang, S.; Goddard, W.; Kalani, M. *J. Phys. Chem. B* **2007**, *111*, 1729–1737.
(36) Gallo, P.; Rovere, M.; Spohr, E. *J. Chem. Phys.* **2000**, *113*, 11324.
(37) Hummer, G.; Rasaiah, J.; Noworyta, J. *Nature* **2001**, *414*, 188–190.
(38) Mashl, R.; Joseph, S.; Aluru, N.; Jakobsson, E. *Nano Lett.* **2003**, *3*, 589–592.
(39) Won, C.; Aluru, N. *J. Am. Chem. Soc.* **2007**, *129*, 2748–2748.
(40) Cicu, P.; Demontis, P.; Spanu, S.; Suffritti, G.; Tilocca, A. *J. Chem. Phys.* **2000**, *112*, 8267.
(41) Fujiyoshi, Y.; Mitsuoka, K.; de Groot, B.; Philippsen, A.; Grubmüller, H.; Agre, P.; Engel, A. *Curr. Opin. Struct. Biol.* **2002**, *12*, 509–515.
(42) Sonoda, M.; Skaf, M. *J. Phys. Chem. B* **2007**, *111*, 11948.
(43) Lin, H.; Van Wagner, E.; Freeman, B.; Toy, L.; Gupta, R. *Science* **2006**, *311*, 639–642.
(44) Smith, G.; Jaffe, R.; Yoon, D. *J. Phys. Chem.* **1993**, *97*, 12752–12759.
(45) Bedrov, D.; Smith, G. *J. Phys. Chem. B* **1999**, *103*, 3791–3796.
(46) Vaiana, A.; Schulz, A.; Wolfrum, J.; Sauer, M.; Smith, J. *J. Comput. Chem.* **2003**, *24*, 632–639.
(47) MacKerell Jr, A.; Banavali, N. *Biopolymers* **2001**, *56*, 257–265.
(48) Berendsen, H.; Grigera, J.; Straatsma, T. *J. Phys. Chem.* **1987**, *91*, 6269–6271.
(49) Borodin, O.; Bedrov, D.; Smith, G. *Macromolecules* **2001**, *34*, 5687–5693.
(50) Widengren, J.; Mets, U.; Rigler, R. *J. Phys. Chem.* **1995**, *99*, 13368–13379.
(51) Schuster, J.; Cichos, F.; Wrachtrup, J.; von Borczyskowski, C. *Single Mol.* **2000**, *1*, 299–305.
(52) Culbertson, M.; Williams, J.; Cheng, W.; Stults, D.; Wiebracht, E.; Kasianowicz, J.; Burden, D. *Anal. Chem.* **2007**, *79*, 4031–4039.
(53) Patra, M.; Karttunen, M. *J. Comput. Chem.* **2004**, *25*, 678–689.
(54) Zheng, J.; Li, L.; Chen, S.; Jiang, S. *Langmuir* **2004**, *20*, 8931–8938.
(55) Padmavathi, N.; Chatterji, P. *Macromolecules* **1996**, *29*, 1976–1979.
(56) Ju, H.; McCloskey, B.; Sagle, A.; Wu, Y.; Kusuma, V.; Freeman, B. *J. Membr. Sci.* **2007**, *307*, 260−267.
(57) Lin, H.; Kai, T.; Freeman, B.; Kalakkunnath, S.; Kalika, D. *Macromolecules* **2005**, *38*, 8381–8393.
(58) Tan, G.; Wang, Y.; Li, J.; Zhang, S. *Polym. Bull.* **2008**, *61*, 91–98.
(59) Datta, A. M.Sc. Thesis, Louisana State University, Baton Rouge, LA, 2007.
(60) Chuichay, P.; Vladimirov, E.; Siriwong, K.; Hannongbua, S.; Rösch, N. *J. Mol. Model.* **2006**, *12*, 885–896.
(61) Lindahl, E.; Hess, B.; van der Spoel, D. *J. Mol. Model.* **2001**, *7*, 306–317.
(62) Nosé, S. *Mol. Phys.* **2002**, *100*, 191–198.
(63) Hoover, W. G. *Phys. Rev. A* **1985**, *31*, 1695–1697.
(64) Parrinello, M.; Rahman, A. *J. Appl. Phys.* **1981**, *52*, 7182–7190.
(65) Bhattacharyya, K.; Bagchi, B. *J. Phys. Chem. A* **2000**, *104*, 10603–10613.
(66) Bagchi, B. *Chem. Rev.* **2005**, *105*, 3197–219.
(67) Fenimore, P.; Frauenfelder, H.; McMahon, B.; Young, R *Proc. Natl. Acad. Sci. U.S.A.* **2004**, *101*, 14408.
(68) Nilsson, L.; Halle, B. *Proc. Natl. Acad. Sci. U.S.A.* **2005**, *102*, 13867–13872.
(69) Hua, L.; Huang, X.; Zhou, R.; Berne, B. *J. Phys. Chem. B* **2006**, *110*, 3704–3711.
(70) Pal, S.; Zhao, L.; Zewail, A. *Proc. Natl. Acad. Sci. U.S.A.* **2003**, *100*, 8113.
(71) Pal, S.; Maiti, P.; Bagchi, B.; Hynes, J. *J. Phys. Chem. B* **2006**, *110*, 26396–26402.
(72) Andreatta, D.; Lustres, J.; Kovalenko, S.; Ernsting, N.; Murphy, C.; Coleman, R.; Berg, M. *J. Am. Chem. Soc.* **2005**, *127*, 7270–7271.
(73) Smith, G.; Bedrov, D. *Macromolecules* **2002**, *35*, 5712–5719.
(74) Bedrov, D.; Borodin, O.; Smith, G. *J. Phys. Chem. B* **1998**, *102*, 5683–5690.
(75) Luzar, A.; Chandler, D. *Phys. Rev. Lett.* **1996**, *76*, 928–931.
(76) Starr, F.; Nielsen, J.; Stanley, H. *Phys. Rev. E* **2000**, *62*, 579–587.
(77) Luzar, A.; Chandler, D. *Nature* **1996**, *379*, 55–57.
(78) Yasunaga, H.; Ando, I. *Polym. Gels Networks* **1993**, *1*, 83–92.
(79) Lobo, V.; Valente, A.; Polishchuk, A.; Geuskens, G. *J. Mol. Liq.* **2001**, *94*, 179–192.
(80) Deschenes, L.; Bout, D. *J. Chem. Phys.* **2002**, *116*, 5850.
(81) Marucci, M.; Pettersson, S.; Ragnarsson, G.; Axelsson, A. *J. Phys. D: Appl. Phys.* **2007**, *40*, 2870–2880.
(82) Gagnon, M.; Bissonnette, P.; Deslandes, L.; Wallendorff, B.; Lapointe, J. *Biophys. J.* **2004**, *86*, 125–133.
(83) Andersson, M.; Axelsson, A.; Zacchi, G. *Int. J. Pharm.* **1997**, *157*, 199–208.
(84) Hannoun, B.; Stephanopoulos, G. *Biotechnol. Bioeng.* **1986**, *28*, 829–835.
(85) Schultz, S.; Solomon, A. *J. Gen. Physiol.* **1961**, *44*, 1189–1199.
(86) Karolin, J.; Geddes, C.; Wynne, K.; Birch, D. *Meas. Sci. Technol.* **2002**, *13*, 21–7.

(87) Amsden, B. *Macromolecules* **1999**, *32*, 874–879.
(88) Amsden, B. *Polymer* **2002**, *43*, 1623–1630.
(89) Mills, R.; Lobo, V. *Self-diffusion in Electrolyte Solutions: A Critical Examination of Data Compiled from the Literature*; Elsevier Publishing Company, New York, 1989.
(90) Flynn, G.; Yalkowsky, S.; Roseman, T. *J. Pharm. Sci.* **1974**, *63*, 479–510.
(91) Koneshan, S.; Lynden-Bell, R.; Rasaiah, J. *J. Am. Chem. Soc.* **1998**, *120*, 12041–12050.
(92) Valente, A.; Polishchuk, A.; Lobo, V.; Geuskens, G. *Eur. Polym. J.* **2002**, *38*, 13–18.
(93) Nightingale, E., Jr. *J. Phys. Chem.* **1959**, *63*, 1381–1387.

JP808145X